

Tsunami Force on Bridge Comparison of Two Wave Types by Experimental Test

Li FU¹, Kenji KOSA², Tatsuo SASAKI³ and Takashi SATO⁴

¹ Graduate Student, Dept. of Civil Engineering, Kyushu Institute of Technology
(804-8550, Sensui 1-1, Tobata, Kitakyushu, Japan)

² Ph.D., Professor, Dept. of Civil Engineering, Kyushu Institute of Technology
(804-8550, Sensui 1-1, Tobata, Kitakyushu, Japan)

³ Senior Engineer, Structural Engineering Division, Nippon Engineering Consultants Co., Ltd
(Currently in the doctoral program at Kyushu Institute of Technology)

⁴ Senior Engineer, Structural Engineering Division, Chodai Co., Ltd.
(Currently in the doctoral program at Kyushu Institute of Technology)

1. INTRODUCTION

The 2011 Tohoku Earthquake, known as the Great East Japan Earthquake as well, occurred at 2:46 p.m (JST) on March 11th with a magnitude 9.0. It was one of the most powerful earthquakes to have hit Japan. Besides that, the earthquake caused an extremely destructive tsunami wave which induced an extensive loss in Tohoku region.

After tsunami damage, the authors carried out a reconnaissance visit to the coast of Tohoku region and observed that many bridge girders in Tohoku region have been washed away by tsunami.

Up until now, from previous research¹⁾, it has been known that the tsunami wave came into two types. As shown in Fig. 1, which illustrates the tsunami wave shape about 1km inland at Wakabayashi ward of Sendai city, the whole tsunami wave was long wave with small water surface gradient of 1/103. At the wave front, the 2~3m high bore wave was observed (Type 1) while at the

area close to coastal line, due to small water surface gradient, the 10~20m high wave like steady flow was found (Type 2). Generally, these two tsunami wave types affected on bridges after tsunami happened.

Corresponding proper design method to above two wave types has not been proposed. Therefore, the authors conducted experiment tests for bore wave and steady flow from 2008 to 2013, in order to find the design method for their tsunami loads on bridge girder.

In this research, the measurement method, parameters and measuring results of wave horizontal forces of two wave types are introduced. Furthermore, the difference of wave horizontal forces between two wave types is studied and the wave force of bore wave is confirmed much larger than steady flow.

2. MEASUREMENT OF BORE WAVE

As illustrated in Fig. 2-(a), the total 41m long, 80cm wide, 125cm high water channel was used for

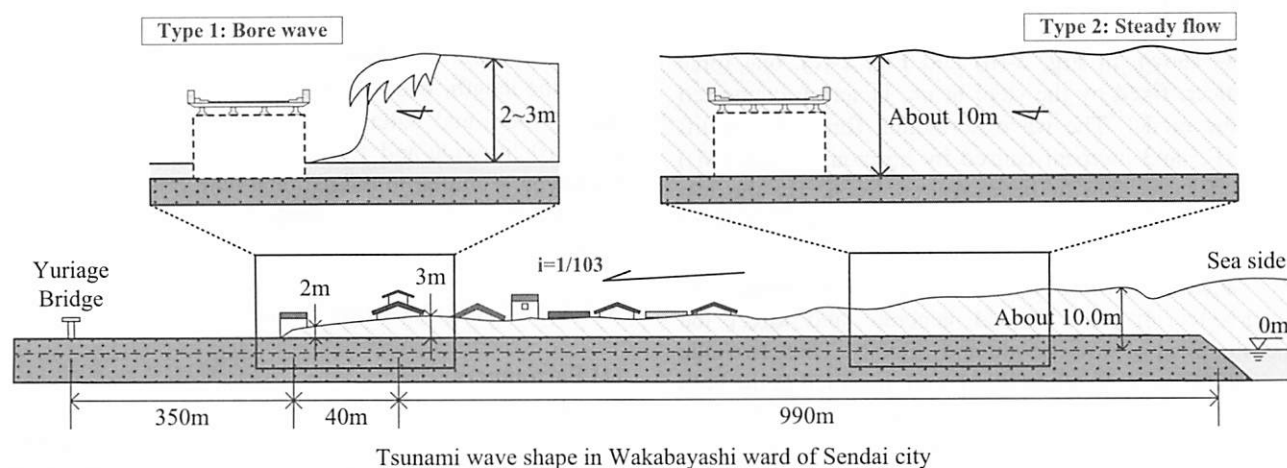


Fig.1 Introduction of Tsunami Wave shapes

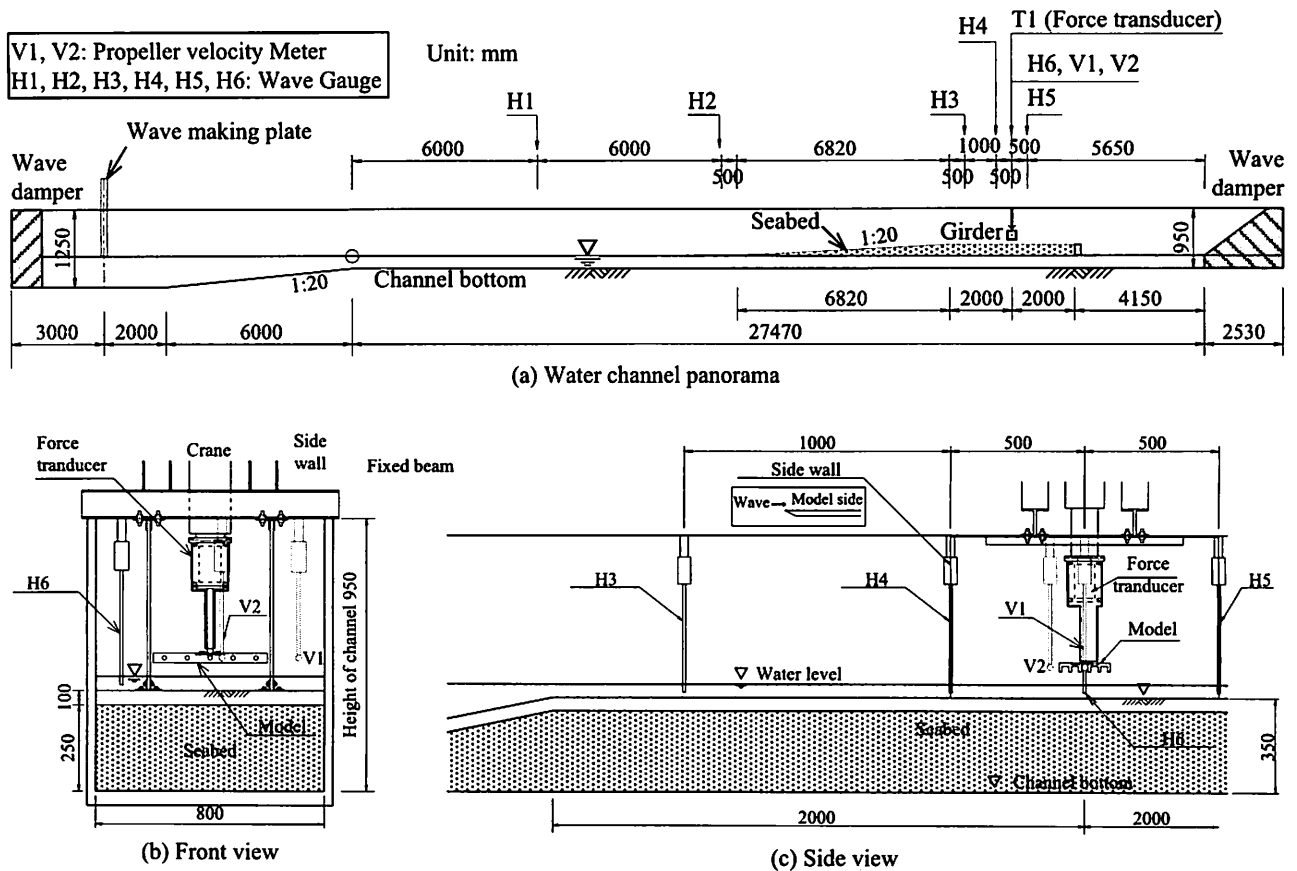


Fig.2 Facility Condition (Bore Wave)

experiment. At the left side of channel, a slide wave making plate is installed to create sine bore wave. From the command of computer, the target wave height is able to be input and created. At the location of girder model, a seabed was set up, which consisted of an inclined plane with the gradient of 1/20.

For the facility settings, six wave gauges (H1~6) were set up along the channel, and H1~5 were used to check the wave shape variation. H6 was set at the center of model location and used to measure the height of a wave just passing through and acting on model.

Two velocity meters (V1~2) were set up at the same height of model to measure the wave velocity. As shown in Fig. 2-(b), V1 was set at the right side of model while V2 was set right ahead of model.

As shown in Fig. 2-(b) and Fig. 2-(c), one force transducer, fixed by the steel beam, is set up connected with the model. The wave horizontal force (F_x), uplift force (F_z) and moment caused by horizontal force (M_y) on model are able to be measured by it. By the test before experiment, it is verified that the natural period of force transducer and model is 30Hz.

When a wave is created and hit on the model, the disturbance of wave would generate and affect the measurement of wave height and velocity. Thus, two side walls (100cm long, 60cm high) were installed at the both sides of model to eliminate the disturbance effect on H6 and V1. Therefore, the output of H6 and V1 would be used to evaluate wave height and velocity.

Moreover, the prototype of girder model is a

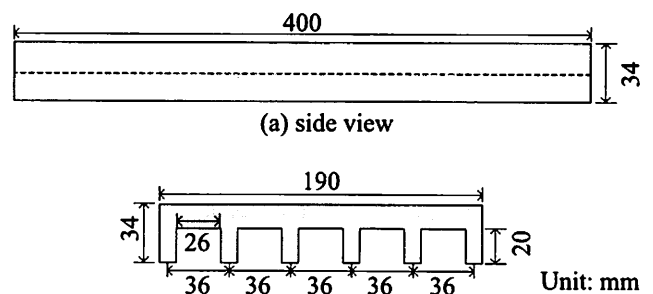


Fig.3 Bridge Girder Model

damaged bridge at Sumatra of Indonesia, due to Indian Ocean Tsunami. As shown in Fig. 3, with the scale of 1/50, the length, width and height of model are made as 40cm, 19cm and 3.4cm respectively (prototype: 19.1m long, 10.2m wide and 1.7m high). Since the size of the prototype is similar to the national road bridges in Japan, the model can be used to evaluate the wave forces on bridges in Tohoku region.

3. EVALUATION FOR BORE WAVE

(1) Parameters

Fig. 4 plots the parameters of experiment for bore wave. Two kinds of parameters are mainly considered: ① wave height (a) ② model position (Z: height from static water level to model bottom).

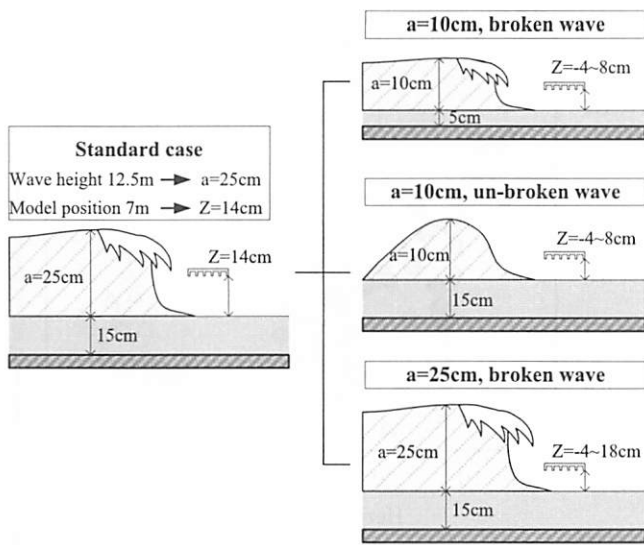


Fig.4 Parameters of Bore Wave Experiment

For the standard case, the 12.5m height of bore wave is intended to reappear and the girder position is considered as 7m. Since the model scale is 1/50, based on the Froude similarity law, the wave height and girder position are converted as 25cm and 14cm in experiment.

Corresponding to the standard case, three patterns of parameter study were conducted as follows:

- Pattern 1: [wave height 10cm, broken wave]
- Pattern 2: [wave height 10cm, un-broken wave]
- Pattern 3: [wave height 25cm, broken wave]

For the three patterns, two kinds of bore wave are able to be created. For pattern 1 and 3, when the original sine wave (created at left end of channel) flowed to the location of model, it would deform and became broken wave. On the other hand, for pattern 2, when the original sine wave flowed to the location of model, it would keep the sine shape, and is called un-broken wave. The broken wave is able to simulate the tsunami wave inland while the un-broken wave can simulate the tsunami wave that just comes to coastal line.

From the comparison of pattern 1 and 2, the difference of wave forces between broken and un-broken waves can be understood. With the study of pattern 1 and 3, the relationship between wave force and wave height can be studied.

(2) Evaluation of Experimental Result

First of all, the experimental result of standard case (a=25cm, Z=14cm, broken wave) is introduced. The graph of Fig. 5 is drawn on the basis of video that records the experimental process and it gives the image of wave impacting on model. It is obvious that the original sine wave became broken wave at model.

The wave shape also can be seen in Fig. 6, which is the time history of wave height (measured by H6, the measuring cycle of output is 1/1000s). It is known that the wave came to model at 9.6s and the maximum wave height was 24.8cm (9.908s). Obviously, the sine wave deformed and formed a great water wall at wave front.

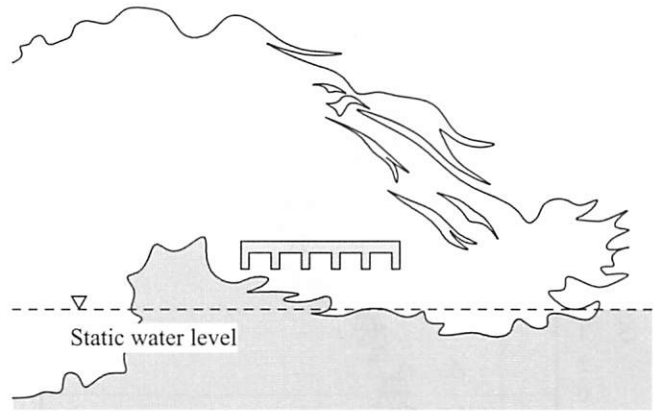


Fig.5 Shape of Bore Wave (Standard Case)

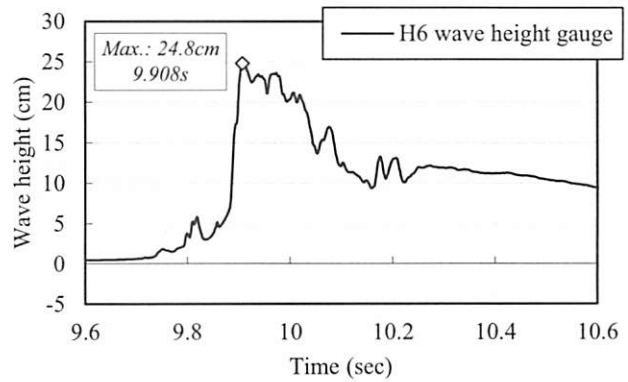


Fig.6 Wave Height (Standard Case)

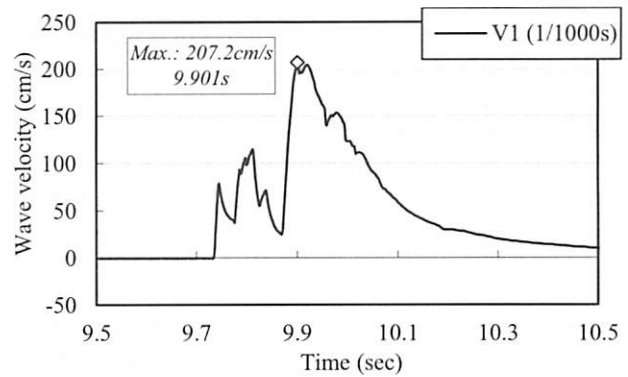


Fig.7 Wave Velocity (Standard Case)

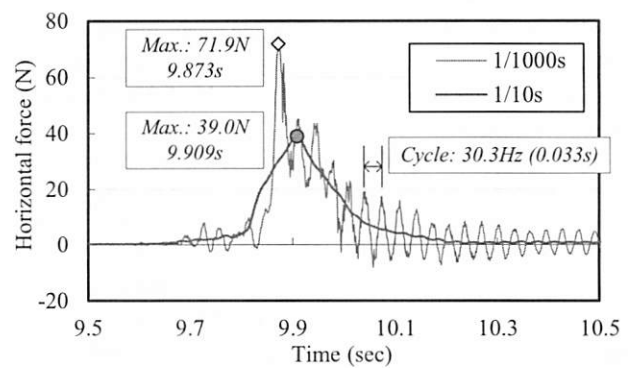


Fig.8 Horizontal Force (Standard Case)

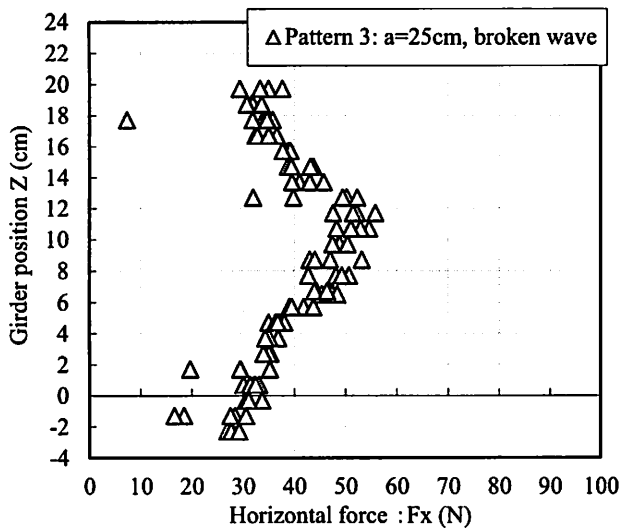


Fig.9 Horizontal Forces (Pattern 3)

After that, the wave velocity time history is given in Fig. 7, and the maximum velocity 207.2cm/s happened at 9.901s. If converted to prototype condition, the maximum wave velocity is calculated as 14.8m/s ($207.2\text{cm/s} \times (50)^{0.5}$), which is a great value.

The time history of wave force due to above broken wave is plotted in Fig. 8. The measuring cycle of original output is 1/1000s and the obvious vibration, the cycle of which is 30Hz, is observed for 1/1000s output. As mentioned in chapter two, the natural period of force transducer and model has been verified as 30Hz, so the vibration of 1/1000s output is caused by resonance possibly. In order to eliminate the effect of resonance, the 1/10s moving average method is applied to consolidate the 1/1000s output. After conducting the 1/10s moving average, the maximum force reduced from 71.9N to 39.0N. In the following evaluation of wave force for other cases, the results after the 1/10s moving average would be concentrated.

The maximum wave forces after moving average of pattern 3 are plotted in Fig. 9. For each case of model position Z, 3~5 times of repeated experiments were carried out, in order to ensure the reasonability of measurement. As a consequence, for most of cases, the repeatability is proved well. If concentrating on the wave force distribution in vertical direction, it is noted that when the model was set at the central height of wave ($Z=12\text{cm}$), the wave force on model was greatest. And when the model was set at the static water surface ($Z=0\text{cm}$), the wave force was about half of that measured at central height.

For the sake of the comparison of wave forces of three patterns, when plotting wave forces, the model position was processed by dimensionless (the model position Z was divided by wave height a). The distribution of wave forces of three patterns after dimensionless is illustrated in Fig .10. In general, the wave forces of pattern 3 are greater than the other two patterns, which demonstrates that the wave force of bore wave would become greater with the increase of wave

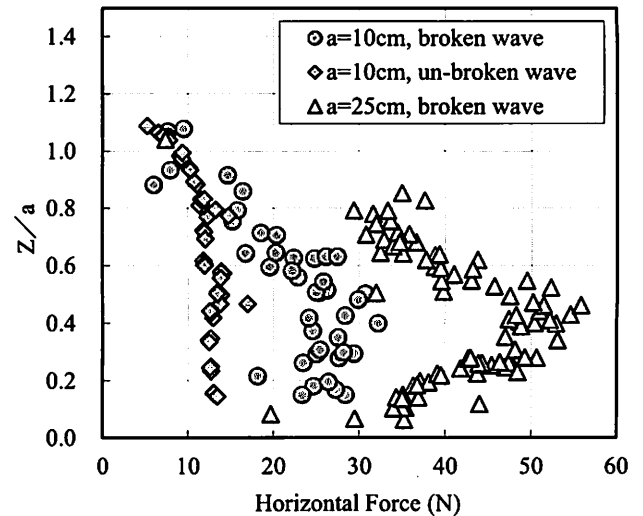


Fig.10 Horizontal Forces of All Cases

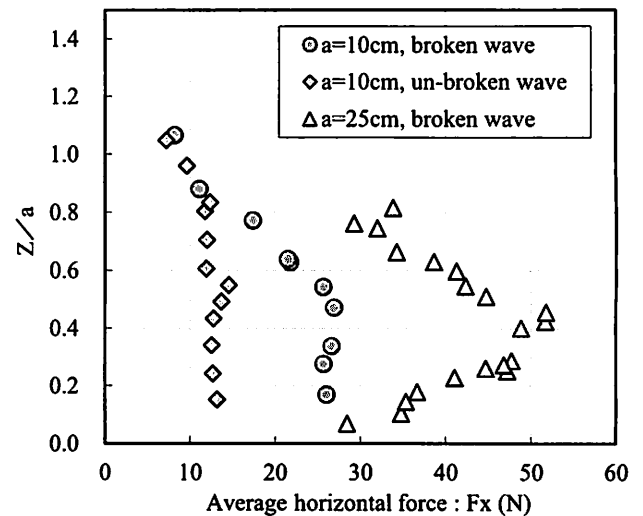


Fig.11 Horizontal Forces of All Cases (Average)

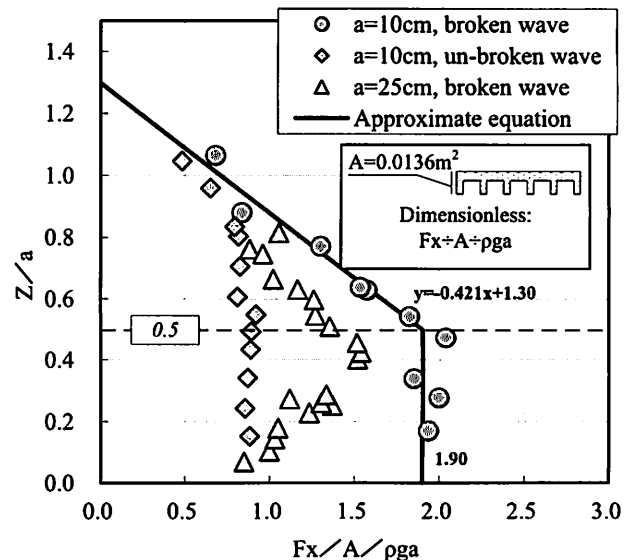


Fig.12 Dimensionless of Horizontal Force

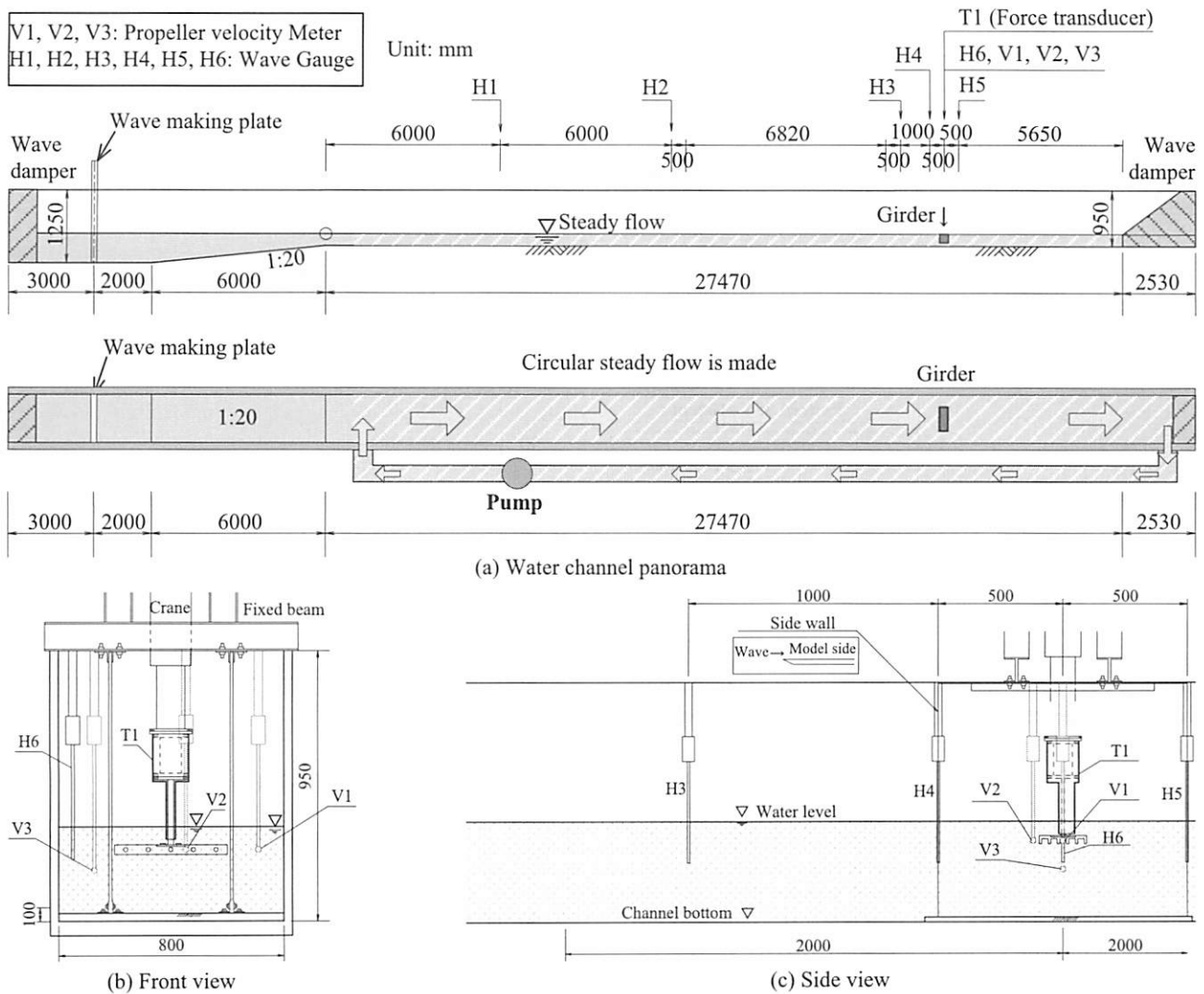


Fig.13 Facility Condition (Steady Flow)

height. Furthermore, it is notable that the wave force of broken wave is stronger than un-broken wave, if the wave heights of them are same by comparing pattern 1 and 2.

Fig. 11 plots the average result of cases for each model position Z . For pattern 1, if the model approached to the position of wave top, the wave force would decrease and if the model was near the static water surface, the wave force would become greater gradually. For pattern 2, although the wave force decreased slightly at wave top, the general trend of wave force of all cases nearly kept a constant (about 13N). For pattern 3, with the $Z/a=0.5$ as the critical value, no matter for $Z/a>0.5$ or $Z/a<0.5$, the wave force would decrease gradually.

Afterwards, the authors conducted dimensionless for wave forces by the method shown in Fig. 12, in order to get the evaluation equations for wave forces. The dimensionless of wave force is performed, divided by side area A of model and the equivalent static water pressure $\rho_w g a$ corresponding to wave height. After dimensionless, the result of pattern 1 shows greatest trend. If defining the $q_x (=F_x/A)$ as the wave pressure, the approximate line for the ratio of wave pressure and equivalent static water pressure can be simulated by Eq.

(1) and (2):

$$Z/a = -0.42q_x / \rho_w g a + 1.30 \quad (Z/a > 0.5) \quad (1)$$

$$q_x / \rho_w g a = 1.9 \quad (Z/a \leq 0.5) \quad (2)$$

In which, a is wave height (m); Z is girder position (m); ρ_w is water density (kg/m^3); g is acceleration of gravity (9.8 m/s^2).

From the wave pressure distribution, it is noted that, if $Z/a > 0.5$, the wave pressure shows triangular distribution and if $Z/a \leq 0.5$, the wave pressure is nearly a constant, which is about 1.9 times as strong as equivalent static water pressure $\rho_w g a$. The Eq. (1) and (2) are suggested to calculate the wave force of bore wave, with wave height and girder position as functions.

4. MEASUREMENT OF STEADY FLOW

The experiment of second wave shape: steady flow was also carried out. As shown in Fig. 13-(a), different from bore wave, the pump of water channel was applied to make a steady circular flow and the flow velocity is able to be controlled by the rotation speed of pump.

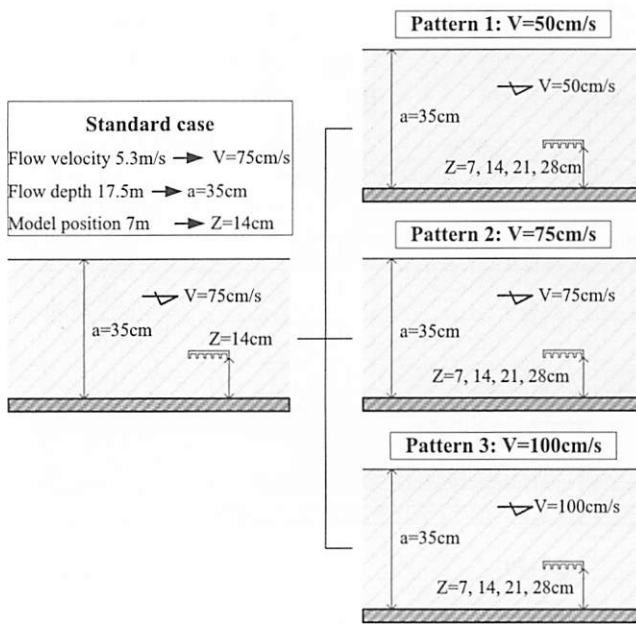


Fig.14 Parameters of Steady Flow Experiment

Besides, in order to make sure the stability of steady flow, the seabed was removed. After inspection, the maximum flow velocity 120cm/s can be got by the pump.

For steady flow, the flow velocity is a significant parameter for the evaluation of force on model. Since the average flow velocity of ideal steady flow happens near the central height, another velocity meter V3 was supplied at the central height of steady flow and the output of V3 would be used to control the parameter of flow velocity (Fig. 13-(a) and Fig. 13-(b)).

Furthermore, same as the measurement of bore wave, the output of H6 and V1 would be applied to evaluate the wave height and velocity of flow that acts on model.

5. EVALUATION FOR STEADY FLOW

(1) Parameters

The steady flow velocity of standard case was set on the basis of the tsunami conditions of Utatsu bridge, Koizumi bridge and Kesen bridge damaged by the tsunami due to Great East Japan Earthquake (For the size of bridge cross section, since the average scale between model and three bridges is about 1/50, so the scale 1/50 also can be used). As plotted in Fig. 14, the average tsunami velocity at three bridges was confirmed as 5.5m/s, thus according to the Froude similarity law, the flow velocity of standard case was set as 75cm/s ($5.5\text{m/s}/(50)^{0.5}$). The standard model position Z was set as 14cm, which is same as the standard case of bore wave. Furthermore, by referring to the maximum inundated depths at three bridges, the 17.5m of flow depth was got and after conversion, the standard flow depth 35cm was applied.

On the basis of standard case, three patterns (V=50, 75, 100cm/s) of parameter cases were proposed. As mentioned previously, the parameter of flow velocity

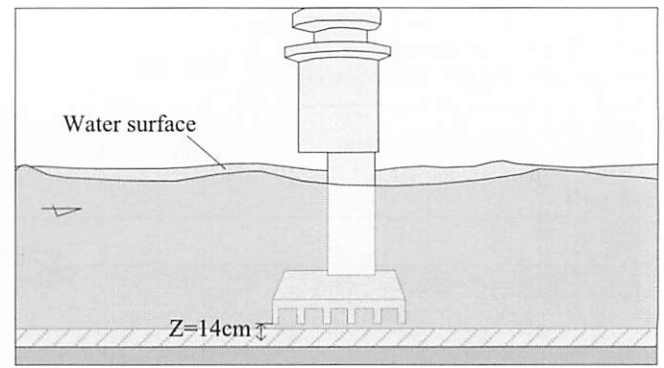


Fig.15 Shape of Steady Flow (Standard Case)

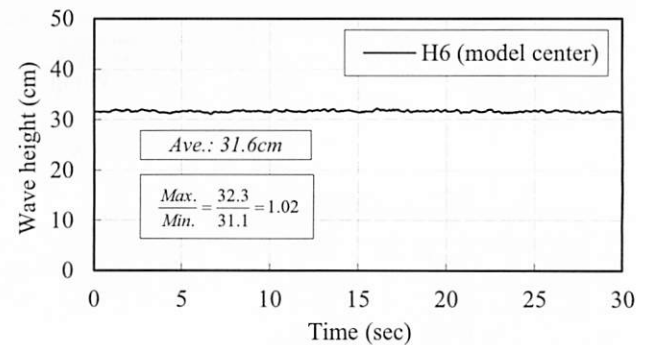


Fig.16 Wave Height (Standard Case)

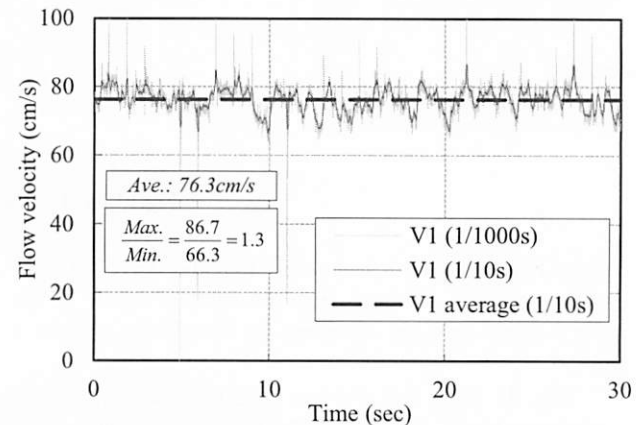


Fig.17 Steady Flow Velocity (Standard Case)

was controlled by the output of V3. For each pattern, the experiment was conducted with four model positions (Z=7, 14, 21, 28cm), in order to check the velocity and wave force distribution at vertical direction. Same as bore wave experiment, for each case, three times of repeated experiments were conducted.

(2) Evaluation of Experimental Result

The result of standard case would be introduced primarily. As shown in Fig. 15, drawn based on the video recording experiment, the flow condition of steady flow can be confirmed.

From the wave height history (1/1000s) by H6 in Fig. 16, it is known that the flow could keep stable condition because the vibration of wave height time

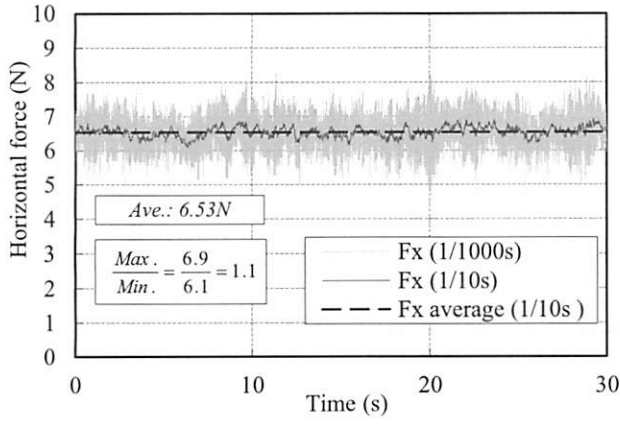


Fig.18 Steady Flow Force

history almost did not happen (max./min.=1.02). Besides, the average wave height is 31.6cm.

Afterwards, the flow velocity time history by V1 is illustrated in Fig. 17. Different from wave height, the original output of 1/1000s generated great vibration due to the electromagnetic noise. Therefore, the 1/10s moving average was applied to eliminate the vibration and the average velocity after 1/10s moving average is 76.3cm/s. Compared with the wave height, the vibration of flow velocity time history is found greater (max./min.=1.3).

What's more, the wave horizontal force time history is given in Fig. 18. Similar to the flow velocity, in order to eliminate the electromagnetic noise, the 1/10s moving average method was used. As a result, the average force is 6.53N, and the data vibration is relatively small (max./min.=1.1). Thus, the average wave force can be used for force evaluation.

If concentrating on the flow velocity distribution in vertical direction of three patterns, as plotted in Fig. 19, it is found that the shapes of three distributions are similar: from flow surface to bottom, the velocity decreased slightly. Furthermore, the velocity in vertical direction almost did not change (velocity at top (Z=28cm) is about 1.1 times as fast as the velocity at bottom (Z=7cm)).

According to the research²⁾, the tsunami force is able to be evaluated by the following Eq. (3):

$$F = \frac{1}{2} \rho_w C_d v^2 A_h \quad (3)$$

Where, F is the tsunami acting force (kN); ρ_w is the sea water density (1.03g/cm³); C_d is the drag coefficient (1.54, determined according to the Japanese Specification³⁾); v is the tsunami velocity (m/s); A_h is the effective projected area on girder (m²).

For steady flow condition, the reasonability of Eq. (3) has been checked. For each case, by substituting the average flow velocity of V1 (such as 76.3cm/s in Fig. 17), into Eq. (3), the average wave force is able to be calculated. The comparison of calculating and measuring wave forces is illustrated in Fig. 20. It is apparent that the wave forces by two ways show the same level for pattern 1 and 2. Thus, the authors suppose that the wave

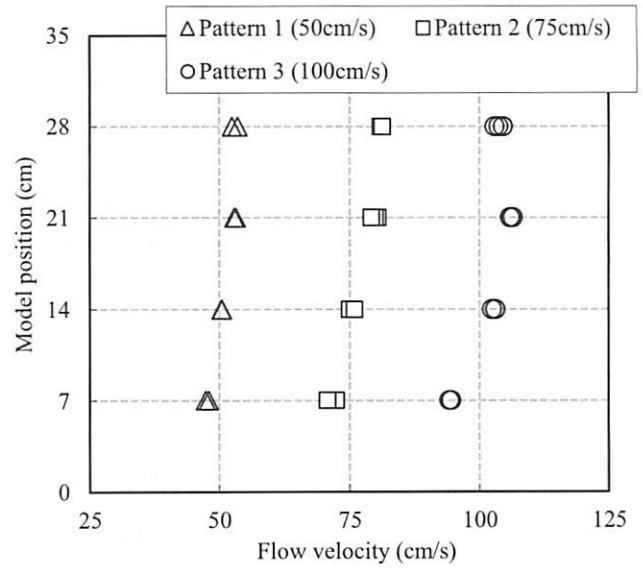


Fig.19 Flow Velocity Distribution (V1)

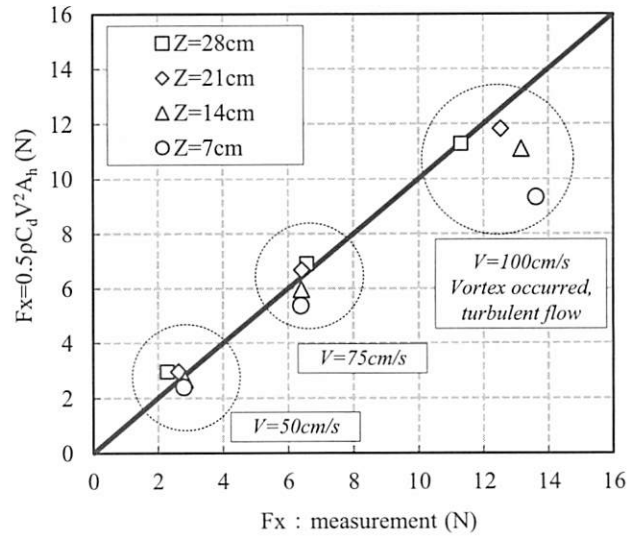


Fig.20 Comparison of Calculating and Measuring Wave Force

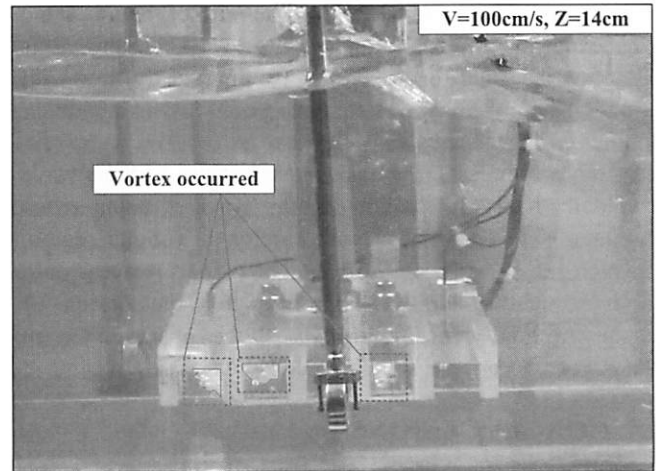


Fig.21 Turbulent Condition of Pattern 3

force of steady flow is mainly decided by flow velocity and nearly has nothing to do with model position Z.

However, for pattern 3, the measurement is greater than calculation and the plotted points distributed dispersedly, although the flow velocities have little difference. In order to find out the reason, the authors checked the flow condition of pattern 3 (Fig. 21). Consequently, it is found that the strong vortexes generated between girders when the flow affected on model, which cannot be observed for pattern 1 and 2. So it is supposed that the flow of pattern 3 begin to change into turbulent condition and is not proper for evaluation of steady flow. In summary, if ignoring the cases of pattern 3 that vortexes generated, the wave forces of steady flow is able to be evaluated by the Eq. (3).

6. COMPARISON OF WAVE FORCES OF TWO WAVE TYPES

According to the experimental results of chapter three and five, the levels of wave forces of bore wave and steady flow are able to be compared roughly.

The wave force comparison of standard cases is plotted in Fig. 22. With the similar wave height (bore wave: 25cm, steady flow: 35cm), the wave force of bore wave (39.0N) is found to be six times as strong as steady flow (6.5N).

In order to understand the wave force level for real tsunami condition. The experimental conditions of standard cases were converted to conditions of prototypes, as shown in Fig. 23. For the conversion of wave force, the conversion rule of Eq. (4) mentioned in the research⁴⁾ was used.

$$\frac{(F_l)_m}{(F_l)_p} = \lambda^3 \quad (4)$$

Where, $(F_l)_m$ and $(F_l)_p$ are wave forces corresponding to experiment and prototype (N); λ is experimental scale 1/50;.

As a result, the wave forces of bore wave and steady flow are 4875kN and 812.5kN. The ratio of them is same as experimental condition ($F_{x1}/F_{x2}=6$). Therefore, it is summarized that for the bore wave and steady flow with similar height, the wave force of bore wave is about six times stronger than steady flow.

Nevertheless, it is also noted that the 14.8m/s wave velocity of 12.5m height of bore wave is about twice greater than observed wave velocity in Tohoku region, which means such a 12.5m height of bore wave would not happen generally. Therefore, for the design of tsunami load due to bore wave, the observed 2~3m height of bore wave should be considered.

7. CONCLUSIONS

From the experimental tests for two tsunami wave types, the following conclusions are summarized:

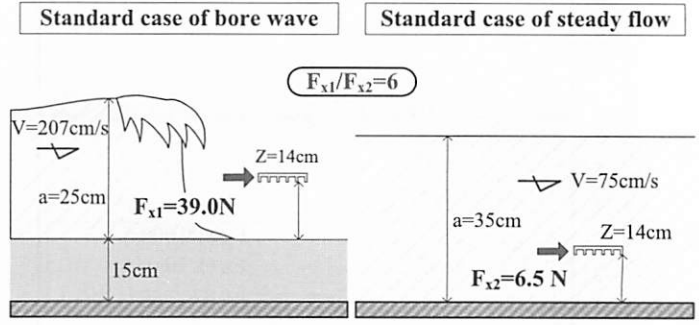


Fig.22 Comparison of Wave Forces for Standard Case

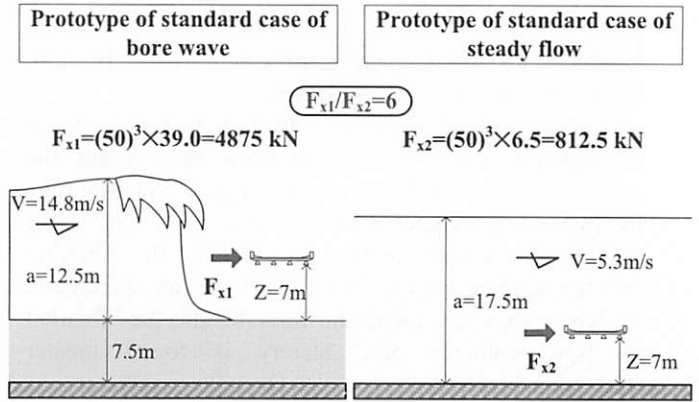


Fig.23 Comparison of Wave Forces for Prototypes of Standard Cases

- (1) From the experiment of bore wave, it is known that the wave force of bore wave is related with wave height and girder position and the approximate evaluation equations can be obtained with the parameters of wave height and girder position.
- (2) From the experiment of steady flow, it is known that the wave force of steady flow has proportional relationship with the flow velocity, and the proposed Eq. (3) can be used to evaluate the wave force of steady flow with the flow velocity as parameter.
- (3) By the wave force comparison of standard cases of bore wave and steady flow, it is concluded that for the bore wave and steady flow with similar height, the wave force of bore wave is about six times stronger than steady flow.

REFERENCES

- 1) Fu, L., Kosa, K., Shi, H., and Zheng, Y., "Damage to Structures due to Tsunami and Evaluation of Tsunami Velocity in Shizugawa", Proc. of JCI, Vol.34, No.2, pp.805-810, 2012.
- 2) Kosa, K., Nii, S., Shoji G., Miyahara K., "Analysis of Damaged Bridge by Tsunami due to Sumatra Earthquake", Journal of Structural Engineering, Vol.55A, pp.456-460, 2010.3.
- 3) Japan Road Association, "Specifications for Highway Bridges Part I Common", pp.52, 2002.3.
- 4) Shimosako, K., "Hydraulic Model Experiment", Concrete Journal, Vol.39, No.9, pp.134-135, 2001.9